Time-Resolved Fourier Transform Infrared Emission Spectroscopy of NH Radical in the $X^3\Sigma^-$ Ground State

Adam Pastorek[1,2], Victoria H.J. Clark[3], Sergei N. Yurchenko[3], Svatopluk Civiš[1,*]

1 – J. Heyrovsky Institute of Physical Chemistry, Czech Academy of Sciences, Dolejškova 2155/3, 18200, Prague 8, Czech Republic
2 – Faculty of Nuclear Sciences and Physical Engineering, Czech Technical University in Prague, Břehová 78/7, 11519, Prague 1, Czech Republic
3 – Faculty of Mathematical and Physical Sciences, University College London, Gower Street, London WC1E 6BT, United Kingdom

** Corresponding author*

Abstract

Rotational-vibrational bands of the imine free radical (NH) in the ground $X^3\Sigma^-$ electronic state have been observed by time resolved Fourier transform spectroscopy in the 1923 - 3571 cm^{-1} spectral region with a microsecond time scale and spectral resolution of 0.02 cm^{-1} for the first time. The radical was produced in two experimental arrangements, firstly, with a pulsed positive column discharge of pure hydrogen and nitrogen mixture and secondly, discharge of nitrogen-ammonia mixture in argon buffer gas. In the manuscript, we describe both methods and compare results. We also perform a bi-temperature (non-LTE) modelling of both spectra of discharge systems and demonstrate a perfect match of experiment and theory.

Theoretical background

NH is a key free radical in atmospheric chemistry of fundamental importance. This radical was first detected in 1893 by Eder[1] by his photographic detection near 336 nm and have been the subject of many subsequent investigations. In 1919, imine radical was found in the solar spectra by Fowler *et al.*[2] and in 1930s by Funke[3] who has assigned the main emission branches of the electronic 0-0 and 1-1 bands of $A^3\Pi$-$X^3\Sigma^-$ system in the 29000 cm^{-1} spectral range. The analysis was greatly improved by the observation of the bands in absorption by Dixon[4] from an electronic spectrum that was for a long time a main source of information on this radical. A more complete review related to electronic spectroscopy can be found in Ram *et al.* (1999)[5] and others (below in text).

There have been many infrared and far infrared studies of NH aimed at extracting precise molecular and hyperfine constants in the ground electronic $X^3\Sigma^-$ state. The first observation of these transitions was 1-0 band by Bernath and Amano in 1982.[6] In 1986 Boudjaadar *et al.*[7] observed the $\Delta v = 1$ sequence up to 5-4 band. Line strengths of rovibrational lines and rotational transitions within the ground electronic state are given by J. Brooke *et al.*[8]

The Doppler-limited rotational spectra of the NH radical in its electronic ground $X^3\Sigma^-$ state and vibrational excited state have been measured using the frequency stabilized Cologne side band spectrometer in the frequency range near 2 THz.[9]

From chemical point of view, focusing mainly on the synthesis of imine radical itself, it is possible to mention the study of K. Stewart,[10] who demonstrated main possibilities of NH radical synthesis in the lab for scientific purposes. Especially, the production of NH by azoimide decay by active nitrogen was highlighted. A newer study of reaction mechanism of NH production was the work of Helden *et al.*, who described the mechanism of formation of NH in hydrogen-nitrogen plasma mixture.[11]

Since the discovery of NH in solar spectra, this radical became quickly important among astrophysicists and new extensive studies, focusing on pure fundamental spectroscopy of NH produced by relatively cool laboratory sources, were published in short time. Among many, a flash photolysis of isocyanic acid,[4] a photolysis of ammonia mixed with an inert gas,[12] UV photolysis of ammonia and consequent resonant fluorescence of NH,[13] electric discharge of hydrogen and nitrogen in a hollow cathode[14] or modern two-photon capture on ammonia in a flow reactor by tuneable laser,[15] could be mentioned.

As was already mentioned above, NH radical finds the highest importance in abundance calculations, especially the nitrogen abundance, in stars and in interstellar space. NH was detected in comets, e.g. comet Cunningham,[16] where it was detected with other radicals like CN, OH and CH. Cometary NH can also be used in calculations of photodissociative lifetime of $A^3\Pi$ transitions of NH to the ground state, as demonstrated by P. Singh.[17] NH can also be found in cool stars, for example HD 122563,[18] a metal-poor star. Rovibronic transitions of NH can be observed on Betelgeuse,[19] the second brightest star in Orion constellation. V. Smith *et al.* found NH in 12 red giants[20] and used to calculate the abundance of carbon, nitrogen, oxygen and other elements. Similar publication was the work of Aoki *et al.*,[21] who studied the high resolution spectra of K and M class giants and correctly highlighted the advantage of nitrogen abundance calculation by use of NH radical spectra in comparison with CN.

The first proof of interstellar existence of NH was the publication by D. Meyer[22] from 1991, which demonstrated presense of this radical in a diffuse cloud around ζ Persei and HD 27778. The spectra of NH radical were recorded in the UV region and were assigned to the well-known $A^3\Pi - X^3\Sigma$ band. Later, in 1997, NH was also found in a diffuse cloud close to ζ Ophiuchi, a bright star approx. 366 lightyears from Earth.[23] Data acquired during this observation effectively disproved the theory of the so-called hot formation of NH, when NH is formed by synthesis of nitrogen and hydrogen with a subsequent formation of atomic hydrogen, and supported the hypothesis of formation of NH on dust grain surface in diffuse molecular clouds as a main source of interstellar NH. This theory was also supported by Weselak *et al.* in 2009.[24]

A possible complex origin of nitrogen in metal-poor stars was a subject to study for Spite *et al.* in 2005.[25] The main goal of this publication was to enlighten possible reaction pathways of the origin of light elements in early stages of our galaxy by calculation of abundance ratios and mixing models, used for the estimation of mixing of various layers of stars. By comparing the data from 35 different stars, the work suggested the abundance of gases on the star surface, which did not undergo any mixing, is in accordance with the composition of gases when the star was formed.

As for any astronomically important specie, also NH radical found its place in many purely theoretical publications. One of the first *ab initio* calculations NH was published in 1970,[26] focusing on determination of the bond length. G. Das *et al.*[27] published five ro-vibrational spectroscopic constants of NH via a Dunham fit.. Ram *et al.*[28] obtained spectroscopic constants

for X $^3\Sigma$ = and A $^3\Pi$ states of NHv ia analysis of the existing experimental data. Theconstants are being improved till now.[8,29,30]

In past 20 years, a new application of NH radical emerged, when it was found to be a relevant medium for the research of magnetic molecular traps.[31] These traps are used for the research of physical behaviour of extremely cold and dense matter. NH radical has to be slowed down to low kinetic energy and therefore is cooled and *vice versa*. A metastable energy state of NH, $a^1\Delta$, is used in such experiments due to its desirable properties. The deceleration of NH is realized e.g. by Stark decelerator[32] or Zeeman decelerator.[33] These experiments, ideally leading to completely slowed NH radicals of high local density, have potential application in quantum computers.

In this work time resolved Fourier transform ro-vibrational spectrum of NH in its ground $X^3\Sigma^-$ electronic state is reported covering the 1923 - 3571 cm^{-1} spectral region.

Experimental arrangement

The spectra were obtained by use of the Bruker IFS 120 HR spectrometer with CaF_2 beam splitter and InSb detector in the range 1800 - 4000 cm^{-1}. The broad spectral region was cut by optical interference filter with transparency in the range of 1923 - 3571 cm^{-1}. For the generation of the electric discharge, we used a positive column discharge cell with an outer glass jacket, cooled by running water and immersed in a water tank. The CaF_2 emission window of the cell and CaF_2 entry window of the spectrometer were used. The spectral resolution was 0.02 cm^{-1}. The time resolution of the whole system can be visualized below.

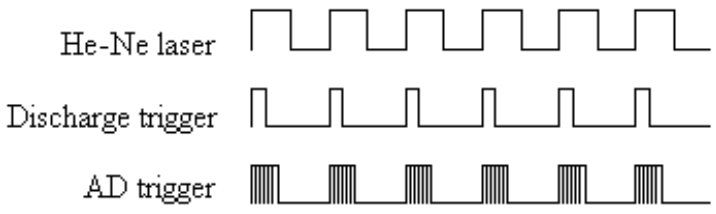

Figure 1: Visualization of the time resolution

As can be seen in Figure 1, a HeNe laser signal is interpreted as a fringe signal, with a length dependent on the speed of mobile mirror of the interferometer itself. Normally, a HeNe laser signal would contain no fringes, but due to passing through the Michelson interferometer and

reflecting from the mobile mirror, interference is created, which produces a cosine-shaped function. By analogue-to-digital conversion, such signal is then processed as fringes by spectrometer. The width of a single HeNe laser fringe is 100 μs, when the speed of the mobile mirror is set to 10 kHz. The discharge trigger, realized by Behlke HTS 81 (Behlke Electronic, Frankfurt, Germany) fast transistor switch, symbolizes how the discharge pulse can be operatively switched according to set parameters. In our measurements, the length of the pulse varied between 22-30 μs. Lastly, the AD trigger stands for the trigger of the data acquisition. By setting of this parameter, it is possible to collect the data before, during or after the discharge pulse and with various time intervals. We used no data acquisition offset (offset stands for a dead time, when all data from the detector are omitted) and collected 30 acquisition data points at each 2nd or 3rd μs, so the acquisition covered 60 or 90 μs.

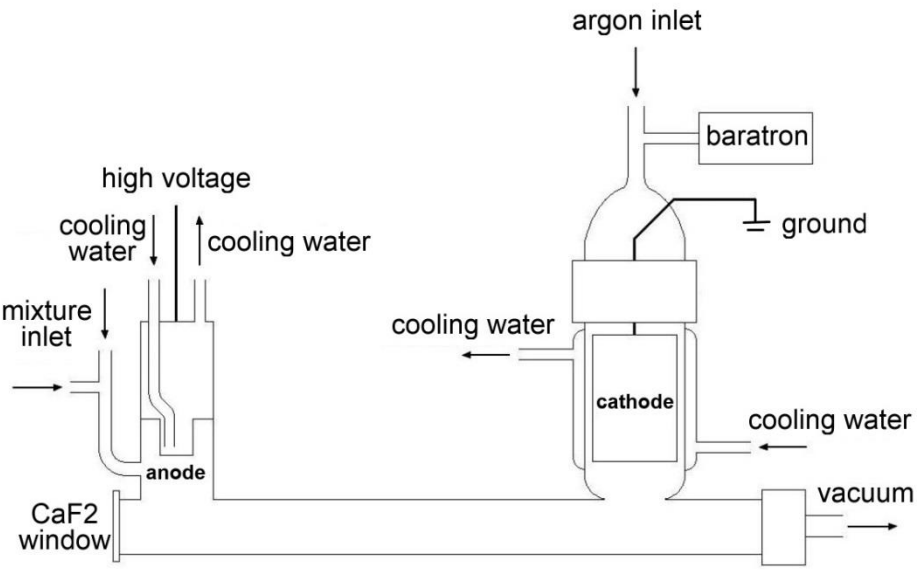

Figure 2: The discharge cell

As can be seen in Figure 2, the discharge cell was 25 cm long and of 12 mm of an inner diameter. The voltage across the both electrodes varied from 1 to 1.4 kV and the electric current was 150-300 mA. The emission radiation from the discharge cell was focused into the aperture of the spectrometer by a CaF_2 lens. The aperture diameter was set to 2 mm.

The discharge was realized either with a mixture of hydrogen and nitrogen (pressure ratio 1:1, total pressure of 3 Torr), or with a mixture of nitrogen and ammonia in argon buffer gas. In the latter, the pressure was 0.5 Torr of argon, 0.8 Torr of nitrogen and 0.1 Torr of ammonia.

Results and discussion

Figure 3 demonstrates the overall spectra of NH radical in 2400-3600 cm^{-1} spectral range.

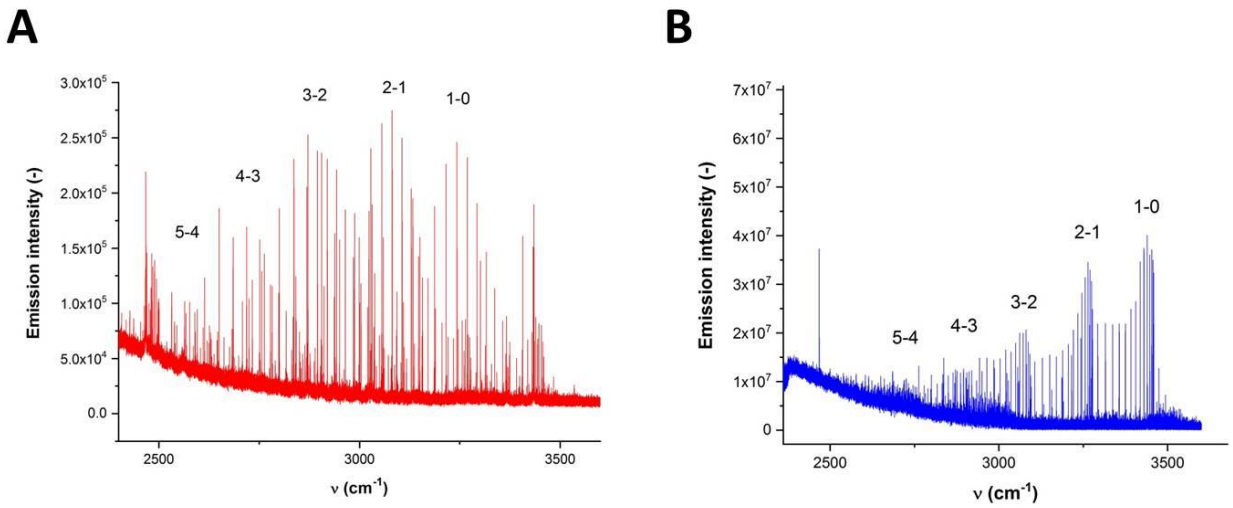

Figure 3: Panel A – averaged spectrum of H_2 + N_2 discharge
Panel B – averaged spectrum of NH_3 + N_2 + Ar discharge

In panel A of Figure 3, the spectrum of the H_2 + N_2 discharge averaged over most intense times is displayed. This spectrum was obtained by collecting50 scans. The bands are marked according to vibrational transitions. The spectrum of the second mixture NH_3 + N_2 + Ar (Panel B) was produced with higher signal-to-noise ratio and a slightly different population of the rotational-vibrational bands. It should be however that the second spectrum was obtained by averaging 100 scans.

The technique presented in this work allows acquiring lifetimes of rotational-vibrational transitions. We have observed rotational-vibrational transitions in the ground electronic state $X^3\Sigma^-$ for the fundamental band and hot bands up to 5-4. The lines of the imine radical and atoms (H, N) were assigned according to the literature. We have evaluated the data for fundamental and hot bands for selected lines from each P and R branch and estimated lifetimes. The results for the several lines of hot bands are given in Table 1.

Table 1: Classification and lifetimes of selected emission lines of the NH radical

ν (cm^{-1})	upper–lower v	upper *N, J*	lower *N, J*	upper level lifetime (μs)
2778.19	4-3 (R)	5; 6	4; 5	30.8 ± 4.2
2532.12	4-3 (P)	4; 3	5; 4	25.9 ± 4.5
2919.73	3-2 (R)	4; 4	3; 3	35.9 ± 2.9
2685.03	3-2 (P)	3; 4	4; 5	37.0 ± 4.6
3081.46	2-1 (R)	4; 5	3; 4	40.6 ± 2.9
2871.51	2-1 (P)	2; 3	3; 4	45.9 ± 4.4

As number of selected lines of NH from the thirty time resolved spectra were integrated and are plotted in Figure 4 as functions of time. . Time profiles of the integral intensity of the 2-1 (3081.46 cm^{-1}) and 1-0 (3242.96 cm^{-1}) as well as of the hydrogen atomic line (4f – 5g, 2467.75 cm^{-1}) are shown as an example in Figure 4.

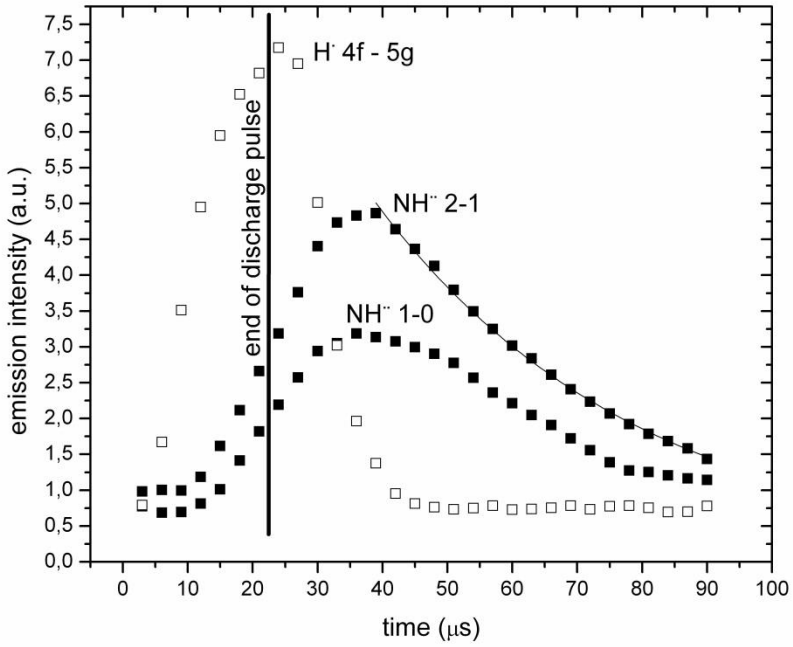

Figure 4: The time profiles of selected lines (NH 2-1 fitted by exponential function) in the $N_2 + H_2$ mixture

The intensity of the NH lines is increasing during the discharge pulse (duration 22 μs) and achieves the maximum at the 39th μs. After that the line intensities of imine radical start to decrease for all transitions. The intensities of nitrogen and hydrogen atomic lines are increasing during the discharge and reaching the maximum at the end of the discharge pulse. The atomic lines in the spectra are disappearing at the 45th μs. The values of the obtained lifetimes (under aforementioned experimental conditions) are summarized in Table 1. The lifetime values of

upper rotational-vibrational levels vary from 20 μs to 50 μs. The lifetimes of transitions from v = 4, v = 3 and v = 2 levels correspond to 26 μs, 36 μs and 46 μs, respectively. The arising tendency of the lifetime values for the lower level is in a good agreement with our previous study of the vibrational relaxation of CN radical in the ground electronic state.[34] The precision of the fit by the first order exponential decay function is reasonable for rotational-vibrational transitions in the hot bands (see Table 1). Our previous experimental knowledge allows to us to compare the line intensities (in the short spectral range) without intensity calibration. We suggest that the mechanism of extinction of excited vibrational states of NH is strongly influenced by collisions at this pressure. The populations of the upper energy levels (v = 5, 4, 3) in comparison with the lower energy levels (v = 1) are much lower with respect to the Boltzmann temperature distribution. The situation in the case of the 1-0 transition is not easy to explain (see the lifetime profile in Figure 3). The intensity of the 1-0 transition is comparable with the intensity of 2-1 transition. The mechanism of extinction of 1-0 band is probably more complicated and decay profile is not possible to be fitted by the first order exponential decay function.

It is possible to observe mutually inverse effect of the emission intensity distribution between nitrogen and NH radical in the N_2 + NH_3 + Ar mixture. Figure 5 below demonstrates the time profiles of selected NH and nitrogen emission lines and their time-resolved spectra.

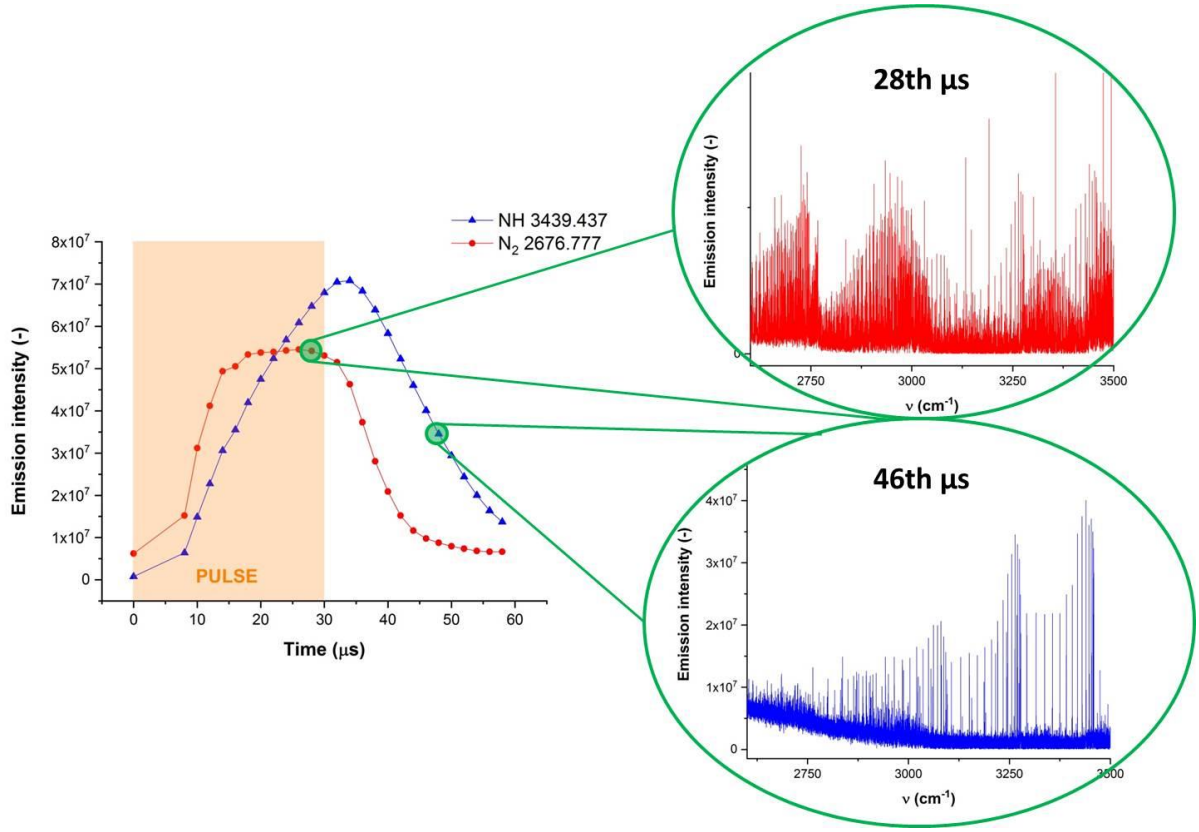

Figure 5: Time profiles of NH and N_2 and the appearance of spectra at specific times

According to the time profile curves in Figure 5, both species appear to gain energy in the discharge pulse (30 μs here). After the pulse, nitrogen starts to lose its energy faster than NH radical, which lives slightly longer as a result of possible mutual energy exchange. At the 28th microsecond, which is still in the discharge pulse, the overall spectrum (in red colour) is depicted in the right top corner of Figure 5. This spectrum is completely occupied by nitrogen and it is difficult to distinguish any NH radical lines here. The right bottom corner of Figure 5 demonstrates the spectrum (in blue colour) of 46th microsecond of the measurement. As can be seen, the spectrum contains no residual nitrogen bands and only NH radical is present. It is very difficult to distinguish NH from nitrogen by use of the non-time-resolved FTIR spectroscopy, since nitrogen covers all other lines due to its omnipresent nature in middle IR region. Nevertheless, by application of time resolution, both species are separated in time and therefore easily recognized in their pure form.

By use of the time-resolved FTIR spectroscopy, we were also able to measure several highly excited pure rotational lines of NH (v = 0). According to our best knowledge, this measurement is one of first experimentally observed pure rotational NH lines with $J>6$ in laboratory by use of cold source.

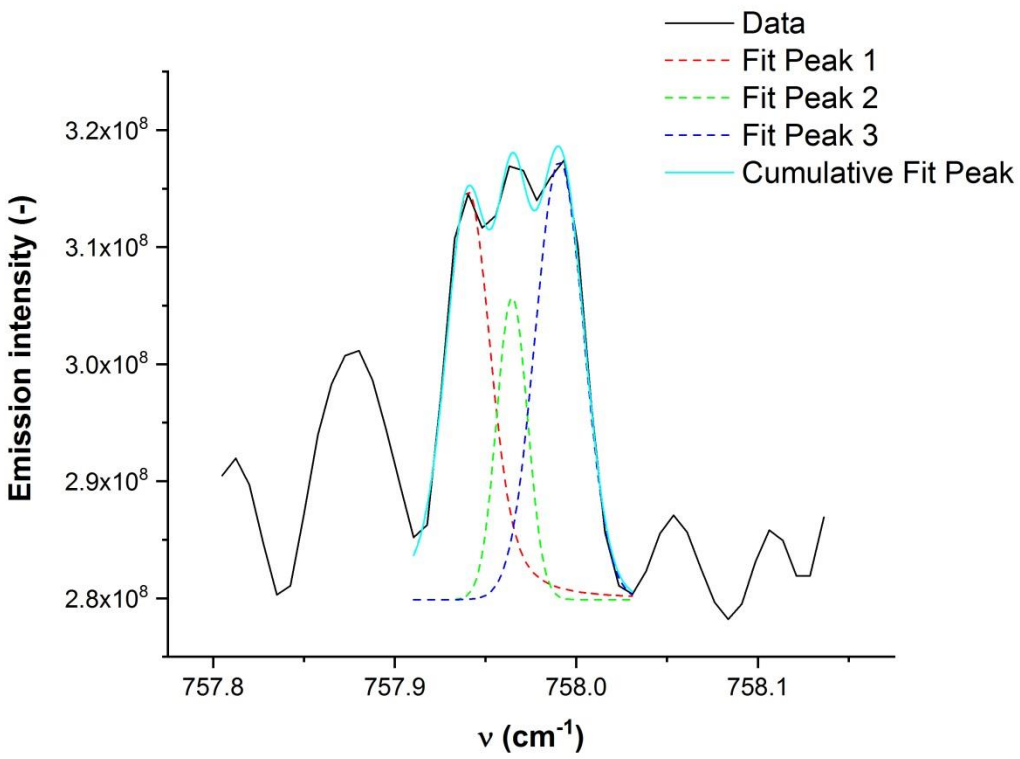

Figure 6: Deconvolution of a NH radical triplet (J'' = 26, v = 0)

As can be seen in Figure 6, pure rotational lines of NH radical are situated in the range of approx. 700-900 cm^{-1} and are resembled in triplets. Our spectral resolution, 0.02 cm^{-1}, was not enough to separate individual peaks and their approximate position had to be estimated by deconvolution of the whole triplet. Our observed pure rotational lines of NH radical can be summarized by Table 1 below.

Table 1: Overview of observed pure rotational NH lines (in cm^{-1})

J''	Our position	Solar position*
26	757.940	757.936
	757.966	757.964
	757.993	757.992
27	776.966	776.966
	776.990	776.986
	777.014	777.009
28	795.104	795.099
	795.125	795.122
	795.146	795.143
29	812.301	812.310
	812.329	812.332
	812.355	812.360

*Solar wavenumbers in Table 1 are extracted from ATMOS (Atmospheric Trace Molecule Spectroscopy) experiment (April 29 – May 2, 1985), described and identified in publications by Farmer and Norton (1989)[35] and Geller *et al*. (1991).[36] For each J'' number a triplet of NH lines is described in Table 1.

With respect to ACE (Atmospheric Chemistry Experiment) data, we compared our NH radical spectra with ACE solar spectra. The match of our and ACE NH lines can be observed in Figure 7.

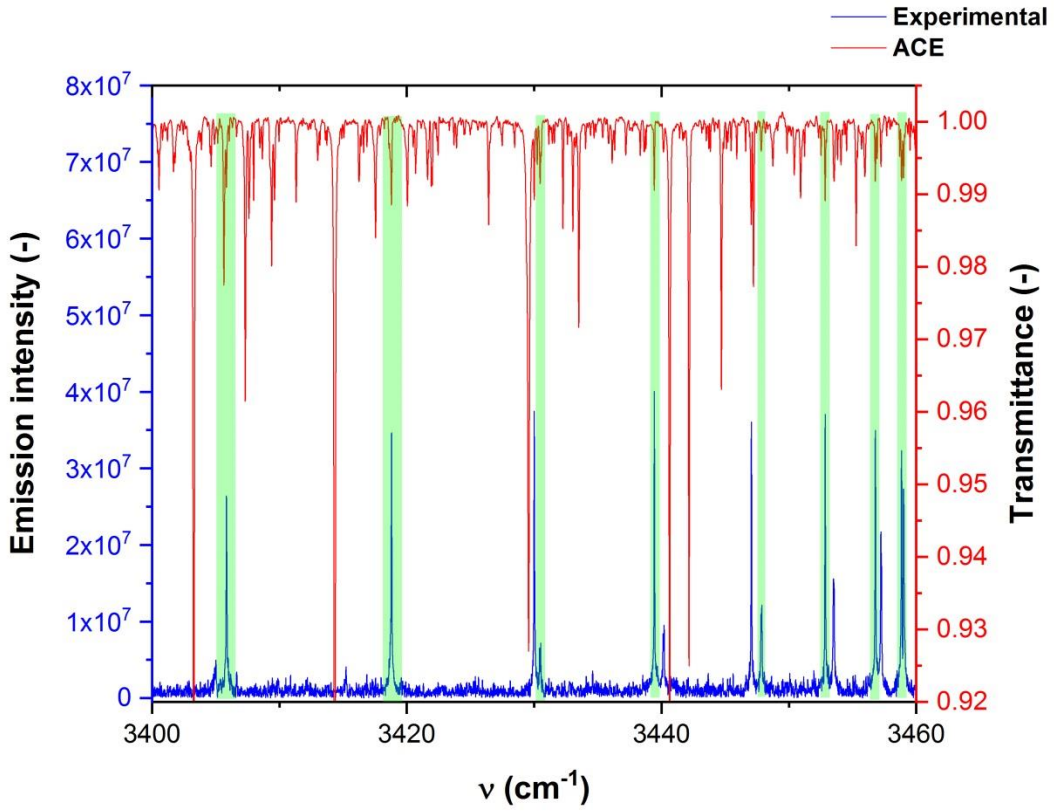

Figure 7: The comparison of ACE solar spectrum and our NH radical data

Figure 7 demonstrates the comparison of our NH radical experimental spectrum with ACE solar spectrum. The coincidences of matching NH lines are highlighted in green colour. The lines depicted in Figure 7 correspond to the 1-0 vibrational band of NH.

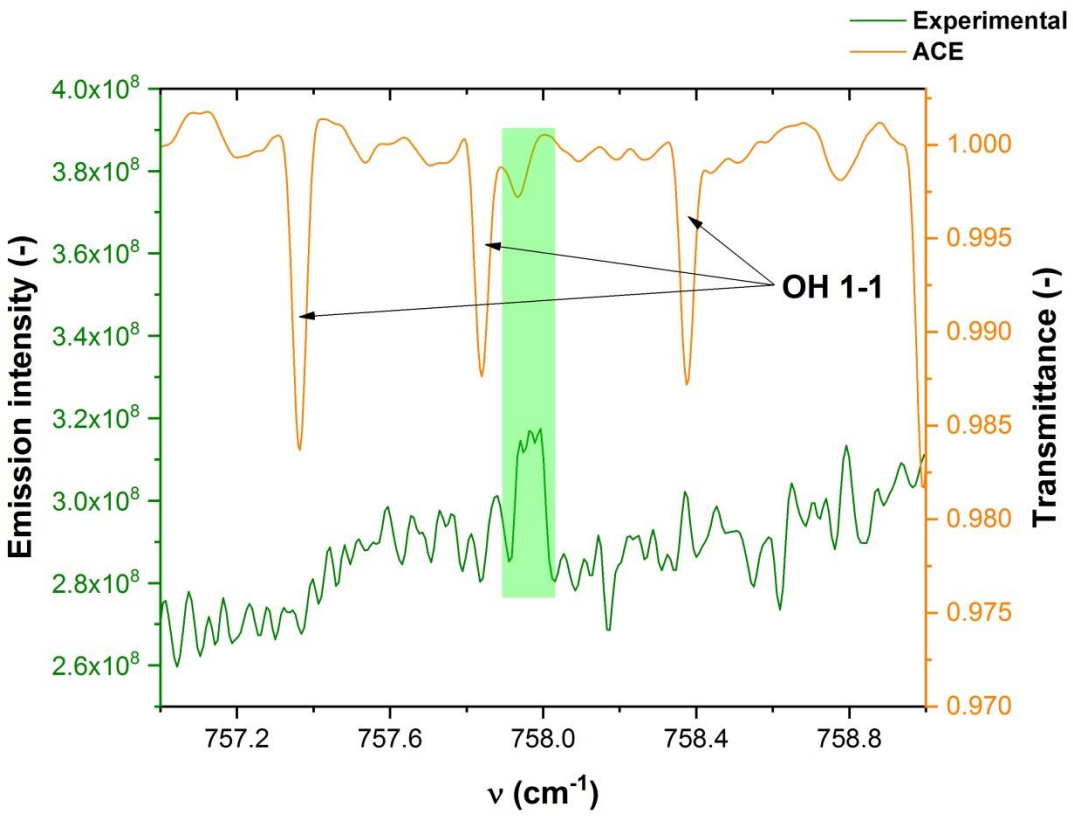

Figure 8: The comparison of ACE solar spectrum with our NH pure rotational triplet

Figure 8 depicts the comparison of ACE solar spectrum with our NH radical pure rotational triplet lines. The coincidence with solar spectrum is highlighted in green colour, but it is possible to see solar spectrum has low population of pure rotational NH lines and they are not even resolved into triplets.

For the information on plasma temperatures, vibrational temperature has been calculated from rotational-vibrational NH bands in the 2700-3500 cm^{-1} range for the N_2 + NH_3 + Ar mixture. Vibrational temperature is given by the linear dependence:

$$\ln\left[\frac{I}{\nu^3(\mathrm{v}'+1)}\right] = KE_{\mathrm{v}'} + Q \qquad (1)$$

where I stands for intensity, ν is the wavenumber of an edge of the selected band (wavenumber of the most intense line), v' is the vibrational quantum number of an upper energy state, K is the slope of the linear regression, $E_{v'}$ is the energy of an upper v-state and Q is a constant. By linear regression of the dependence (1), the vibrational temperature is expressed by:

$$T_V = -\frac{hc}{kK} \tag{2}$$

where *k* is Boltzmann constant.

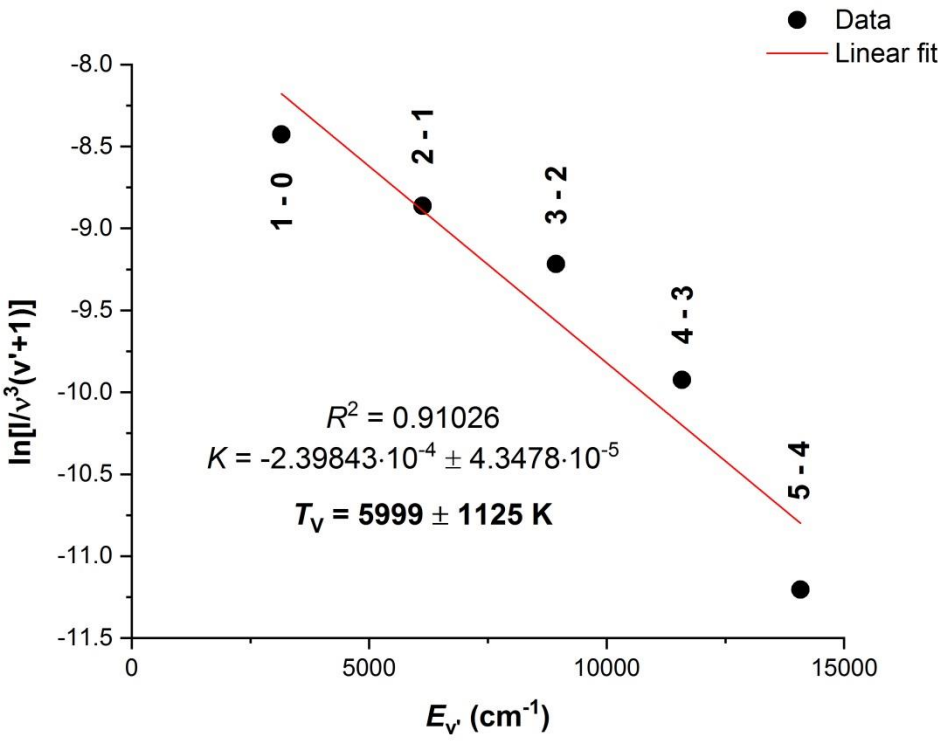

Figure 9: Estimation of vibrational temperature (v-transitions specified)

Vibrational temperature was calculated to be T_V = 5999 ± 1125 K. The J' number was fixed at J' = 4 for all v-transitions.

Non-LTE modelling

Methodology:

The NH cross sections were computed using the MoLLIST line list[8,29,30,37] as provided by ExoMol[38] generated using the program ExoCross.[39] For the non-LTE calculations a bi-temperature approach was used, with separate rotational and vibrational temperatures specified within the spectra. This method is based on the Treanor distribution[40] for energy level population, with rotational and vibrational states described by the corresponding LTE distributions. The separate temperatures for rotations and vibrations are used to calculate the

respective energies, and the total energy is approximated as the sum of the rotational and vibrational energies:

$$\tilde{\mathrm{E}}_{J,\nu} = \tilde{\mathrm{E}}_{\nu}^{vib} + (\tilde{\mathrm{E}}_{J,\nu} - \tilde{\mathrm{E}}_{\nu}^{vib}) \tag{3}$$

where ν and k are the vibrational and rotational quantum numbers, respectively and $\tilde{\mathrm{E}}_{J}^{\nu,rot} = \tilde{\mathrm{E}}_{J,\nu} - \tilde{\mathrm{E}}_{\nu}^{vib}$ is the rotational energy contribution.

The non-LTE distribution of the spectrum then arises from the product of the vibrational and rotational distributions.[39,41]

$$N_{J,\nu}(T_{\mathrm{v}}, T_{\mathrm{R}}) = g_J \frac{e^{-c_2 \tilde{\mathrm{E}}_{\nu}^{vib}/T_{\mathrm{v}}} e^{-c_2 \tilde{\mathrm{E}}_{J}^{\nu,rot}/T_{\mathrm{R}}}}{Q(T)} \tag{4}$$

where $c_2 = hc/k_B$ is the second radiation constant, $\tilde{\mathrm{E}} = \mathrm{E}/hc$ is the energy term value, $g_J = g_J^{ns}\,(2J+1)$ is the state degeneracy, g_J^{ns} is the nuclear-spin statistical weight factor and T_{v} and T_{R} are the vibration and rotation temperatures, respectively. In Eq. (4), $Q(T)$ is the non-LTE partition function defined as a sum over states:

$$Q(T) = \sum g_n^{ns}(2J_n + 1) N_{J,\nu,k}(T_{\mathrm{v}}, T_{\mathrm{R}}) \tag{5}$$

J_n is the corresponding total angular momentum.

An emission line intensity I_{if} (in photon/s) for a transition $i \rightarrow f$ with the wavenumber $\tilde{\nu}_{if}$ is then given by

$$I(i \rightarrow f) = N_{J',\nu',k'} A(i \rightarrow f) \tag{6}$$

where A_{if} is the Einstein-*A* coefficient,

Results:

An LTE emission spectrum of NH obtained from the NH_3 + N_2 + Ar mixture was computed using the ExoMol line list MoLLIST[37,38] and is shown in Figure 10 (bottom) compared to the experimental spectra (top) for the 2500–3500 cm^{-1} range.

Calculations were performed in emission with the LTE temperature T_{V} = 6000 K, which provided the best reproduction of the experimental spectrum, see Figure 10.

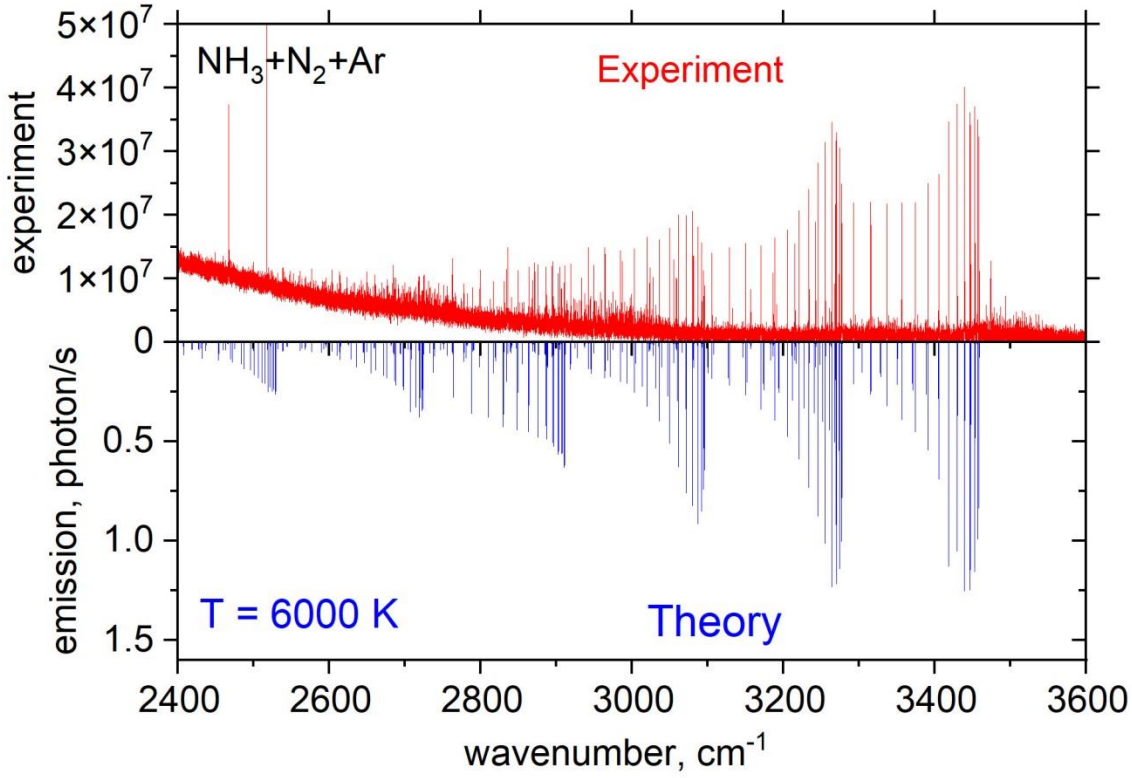

Figure 10: Experiment (red) versus theory (blue) modelling of the NH spectra between 2500-3500 cm^{-1} obtained from the NH_3 + N_2 + Ar mixture. The theoretical spectrum corresponds to T_V = 6000 K and T_R = 500 K, Lorentzian line profile and a HWHM = 0.05 cm^{-1}. The MoLLIST[37,38] line list was used

A non-LTE emission spectrum of NH obtained from the H_2 + N_2 + He mixture was computed for the 2400–3600 cm^{-1} range and is shown in Figure 11 where it is compared to the experimental spectra. Calculations were performed in emission using the ExoMol line list MoLLIST.[37,38] The best agreement with the experiment was achieved for T_R = 500 K and T_v = 8000 K as the rotational and vibrational temperatures, respectively.

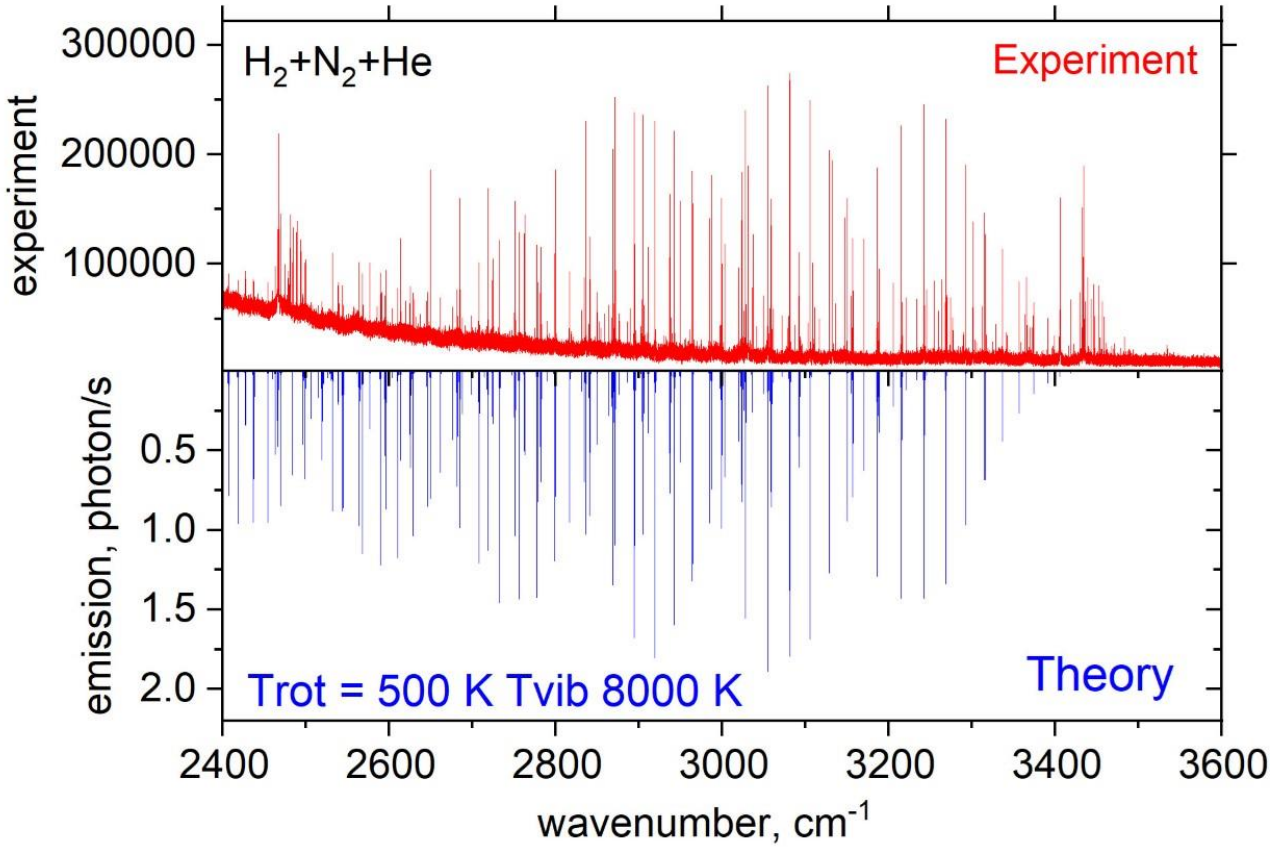

Figure 11: Experiment (red) versus bi-temperature (blue) modelling of the NH spectra between 2400-3600 cm^{-1} obtained from the H_2 + N_2 + He mixture. The theoretical spectrum corresponds to the non-LTE combination of T_R = 500 K, T_v = 8000 cm^{-1}, Lorentzian line profile and a HWHM = 0.02 cm^{-1}. The MoLLIST[37,38] line list was used

Conclusion

We performed time-resolved Fourier transform infrared emission spectroscopy of NH radical in hydrogen-nitrogen mixture and in nitrogen-ammonia-argon mixture. By use of the analysis of time profiles of several lines of NH, we estimated lifetimes of these transitions. The lifetimes decrease with increasing vibrational quantum number, which is in accordance with our previous discovery of the same trend in CN radical spectra. We have also demonstrated our NH radical lines can be found in solar spectra by matching our lines with ACE data. In addition, we presented 4 NH pure rotational triplets in the 750-812 cm^{-1} range, which is one of first experimental observations of $\Delta v = 0$ transitions in the laboratory by use of cold lab source.

Experimentally obtained spectra were theoretically modelled by use of the bi-temperature (non-LTE) approach.

The average vibrational temperature of the discharge plasma in the $NH_3 + N_2 + Ar$ glow discharge mixture, calculated via rovibrational bands of NH radical, was found to be $T_V = 5999 \pm 1125$ K, which is in perfect agreement with our theoretical non-LTE model (see Figure 10).

Acknowledgments

This work was funded by grant no CZ.02.1.01/0.0/0.0/16_019/0000778 alias “ERDF/ESF Centre of Advanced Applied Sciences”. This work was supported by UK research councils EPSRC, under grant EP/N509577/1, and STFC, under grant ST/R000476/1. This work made extensive use of the STFC DiRAC HPC facility supported by BIS National E-infrastructure capital grant ST/J005673/1 and STFC grants ST/H008586/1 and ST/K00333X/1. We thank the European Research Council (ERC) under the European Unions Horizon 2020 research and innovation programme through Advance Grant number 883830.

References

1. Eder, J. M. Beiträge zur Spectralanalyse. *Denksch. Wien. Akad.* **60**, 1–12 (1893).

2. Fowler, A. & Gregory, C. C. L. The Ultra-Violet Band of Ammonia, and Its Occurrence in the Solar Spectrum. *Philos. Trans. R. Soc. London* **218**, 351–372 (1919).

3. Funke, G. W. Das Absorptionsspektrum des NH. *Zeitschrift für Phys.* **101**, 104–112 (1936).

4. Dixon, R. N. The0–0 and 1–0 bands of the A $^3\Pi$–X $^3\Sigma^-$ system of NH. *Can. J. Phys.* **37**, 1171–1186 (1959).

5. Ram, R. S., Bernath, P. F. & Hinkle, K. H. Infrared emission spectroscopy of NH: Comparison of a cryogenic echelle spectrograph with a Fourier transform spectrometer. *J. Chem. Phys.* **110**, 5557–5563 (1999).

6. Bernath, P. F. & Amano, T. Difference frequency laser spectroscopy of the v = 1 ← 0 transition of NH. *J. Mol. Spectrosc.* **95**, 359–364 (1982).

7. Boudjaadar, D., Brion, J., Chollet, P., Guelachvili, G. & Vervloet, M. Infrared emission spectra of five Δv = 1 sequence bands of the free radical NH in its X3Σ- state. *J. Mol. Spectrosc.* **119**, 352–366 (1986).

8. Brooke, J. S. A., Bernath, P. F., Western, C. M., van Hemert, M. C. & Groenenboom, G. C. Line strengths of rovibrational and rotational transitions within the X3Σ− ground state of NH. *J. Chem. Phys.* **141**, 054310 (2014).

9. Lewen, F., Brünken, S., Winnewisser, G., Šimečková, M. & Urban, Š. Doppler-limited rotational spectrum of the NH radical in the 2 THz region. *J. Mol. Spectrosc.* **226**, 113–122 (2004).

10. Stewart, K. The imine radical, NH. *Trans. Faraday Soc.* **41**, 663 (1945).

11. Van Helden, J. H. *et al.* Production mechanisms of NH and NH2 radicals in N 2-H2 plasmas. *J. Phys. Chem. A* **111**, 11460–11472 (2007).

12. Mantei, K. A. & Bair, E. J. Reactions of nitrogen-hydrogen radicals. III. Formation and disappearance of NH radicals in the photolysis of ammonia. *J. Chem. Phys.* **49**, 3248–3256 (1968).

13. Hansen, I., Hoinghaus, K., Zetzsch, C. & Stuhl, F. Detection of NH (X p3Σ−) by resonance fluorescence in the pulsed vacuum uv photolysis of NH3 and its application to reactions of NH radicals. *Chem. Phys. Lett.* **42**, 370–372 (1976).

14. Brazier, C. R., Ram, R. S. & Bernath, P. F. Fourier transform spectroscopy of the A3Π-X3Σ- transition of NH. *J. Mol. Spectrosc.* **120**, 381–402 (1986).

15. Clement, S. G., Ashfold, M. N. R., Western, C. M., Johnson, R. D. & Hudgens, J. W. Triplet excited states of the NH(ND) radical revealed via two photon resonant multiphoton ionization spectroscopy. *J. Chem. Phys.* **96**, 5538–5540 (1992).

16. Swings, P., Elvey, C. T. & Babcock, H. W. The Spectrum of Comet Cunningham, 1940C. *Astrophys. J.* **94**, 320 (1941).

17. Singh, P. D. & Gruenwald, R. B. The photodissociation lifetimes of the NH radical in comets. *Astron. Astrophys.* **178**, 277–282 (1987).

18. Sneden, C. The nitrogen abundance of the very metal-poor star HD 122563. *Astrophys. J.* **184**, 839 (1973).

19. Lambert, D. L., Brown, J. A., Hinkle, K. H. & Johnson, H. R. Carbon, nitrogen, and oxygen abundances in Betelgeuse. *Astrophys. J.* **284**, 223 (1984).

20. Smith, V. V. & Lambert, D. L. The chemical composition of red giants. II - Helium burning and the s-process in the MS and S stars. *Astrophys. J.* **311**, 843 (1986).

21. Aoki, W. & Tsuji, T. High resolution infrared spectroscopy of CN and NH lines: nitrogen abundance in oxygen-rich giants through K to late M. *Astron. Astrophys.* **328**, 175–186 (1997).

22. Meyer, D. M. & Roth, K. C. Discovery of interstellar NH. *Astrophys. J.* **376**, L49 (1991).

23. Crawford, I. A. & Williams, D. A. Detection of interstellar NH towards ζ Ophiuchi by means of ultra-high-resolution spectroscopy. *Mon. Not. R. Astron. Soc.* **291**, (1997).

24. Weselak, T., Galazutdinov, G. A., Beletsky, Y. & Krełowski, J. Interstellar NH molecule in translucent sightlines. *Mon. Not. R. Astron. Soc.* **400**, 392–397 (2009).

25. Spite, M. *et al.* First stars VI - Abundances of C, N, O, Li, and mixing in extremely

metal-poor giants. Galactic evolution of the light elements. *Astron. Astrophys.* **430**, 655–668 (2005).

26. Claxton, T. A. Ab initio UHF calculations. Part 3.—NH radicals. *Trans. Faraday Soc.* **66**, 1540–1543 (1970).

27. Das, G., Wahl, A. C. & Stevens, W. J. Ab initio study of the NH radical. *J. Chem. Phys.* **61**, 433–434 (1974).

28. Ram, R. S. & Bernath, P. F. Revised molecular constants and term values for the X $^3\Sigma$ = and A $^3\Pi$ states of NH. *J. Mol. Spectrosc.* **260**, 115–119 (2010).

29. Brooke, J. S. A., Bernath, P. F. & Western, C. M. Note: Improved line strengths of rovibrational and rotational transitions within the X $^3\Sigma^-$ ground state of NH. *J. Chem. Phys.* **143**, 026101 (2015).

30. Fernando, A. M., Bernath, P. F., Hodges, J. N. & Masseron, T. A new linelist for the $A^3\Pi$–$X^3\Sigma^-$ transition of the NH free radical. *J. Quant. Spectrosc. Radiat. Transf.* **217**, 29–34 (2018).

31. van de Meerakker, S. Y. T., Jongma, R. T., Bethlem, H. L. & Meijer, G. Accumulating NH radicals in a magnetic trap. *Phys. Rev. A - At. Mol. Opt. Phys.* **64**, 4 (2001).

32. Van De Meerakker, S. Y. T., Labazan, I., Hoekstra, S., Küpper, J. & Meijer, G. Production and deceleration of a pulsed beam of metastable NH (a 1Δ) radicals. *J. Phys. B At. Mol. Opt. Phys.* **39**, (2006).

33. Plomp, V., Gao, Z., Cremers, T. & Van De Meerakker, S. Y. T. Multistage Zeeman deceleration of NH X Σ - 3 radicals. *Phys. Rev. A* **99**, 1–6 (2019).

34. Civiš, S., Šedivcová-Uhlíková, T., Kubelík, P. & Kawaguchi, K. Time-resolved Fourier transform emission spectroscopy of A $^2\Pi$-X $^2\Sigma^+$ infrared transition of the CN radical. *J. Mol. Spectrosc.* **250**, 20–26 (2008).

35. Farmer, C. B. & Norton, R. H. A high-resolution atlas of the infrared spectrum of the sun and the earth atmosphere from space. A compilation of ATMOS spectra of the region from 650 to 4800 cm-1 (2.3 to 16 microns). *NASA Ref. Publ. 1224* **2**, (1989).

36. Geller, M., Sauval, A. J., Grevesse, N., Farmer, C. B. & Norton, R. H. First

identification of pure rotation lines of NH in the infrared solar spectrum. *Astron. Astrophys.* **249**, 550–552 (1991).

37. Bernath, P. F. MoLLIST: Molecular Line Lists, Intensities and Spectra. *J. Quant. Spectrosc. Radiat. Transf.* **240**, (2020).

38. Wang, Y., Tennyson, J. & Yurchenko, S. N. Empirical line lists in the ExoMol database. *Atoms* **8**, (2020).

39. Yurchenko, S. N., Al-Refaie, A. F. & Tennyson, J. ExoCross: a general program for generating spectra from molecular line lists. *Astron. Astrophys.* **614**, A131 (2018).

40. Treanor, C. E., Rich, J. W. & Rehm, R. G. Vibrational relaxation of anharmonic oscillators with exchange-dominated collisions. *J. Chem. Phys.* **48**, 1807–1813 (1968).

41. Pannier, E. & Laux, C. O. RADIS: A nonequilibrium line-by-line radiative code for CO_2 and HITRAN-like database species. *J. Quant. Spectrosc. Radiat. Transf.* **222**–**223**, 12–25 (2019).